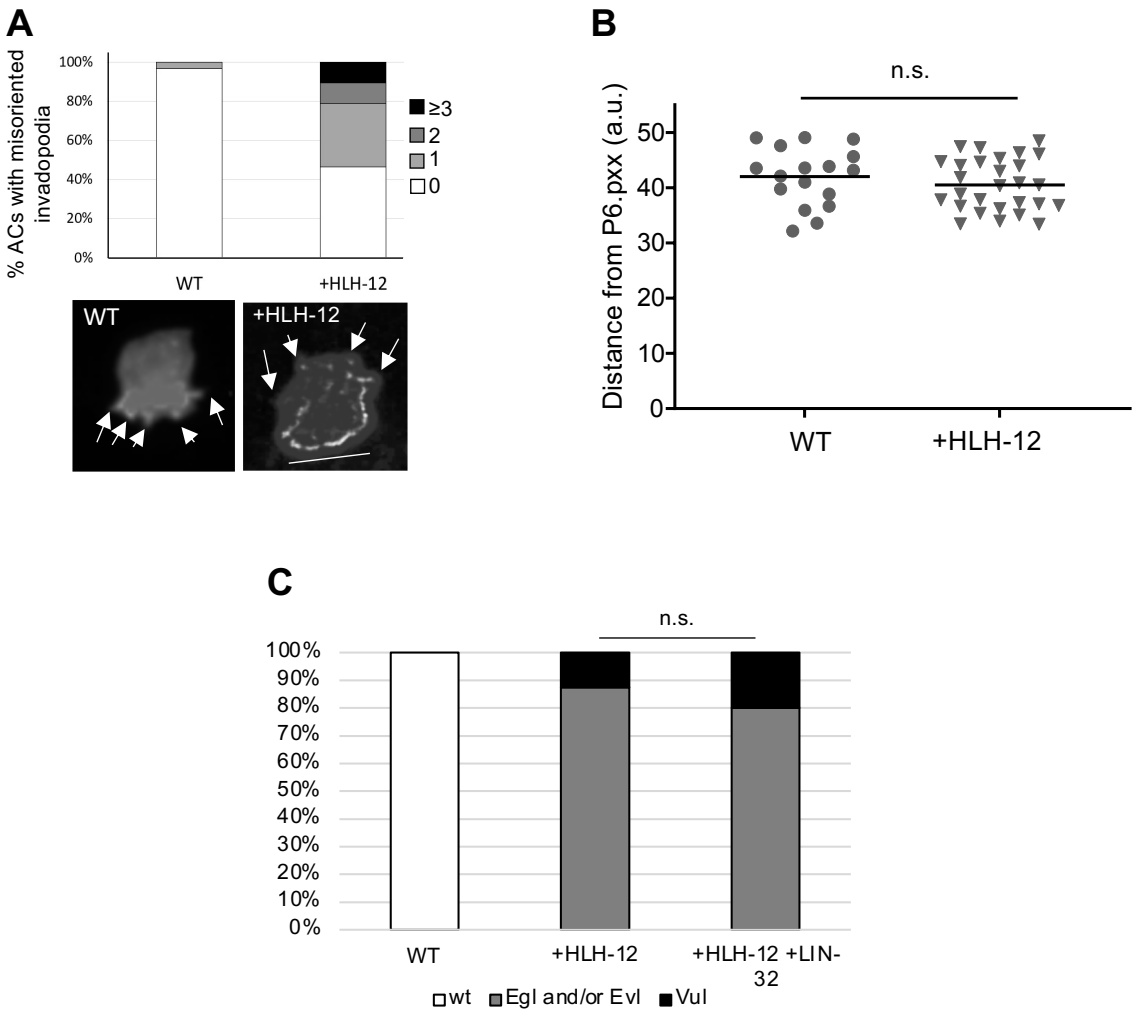

Figure S1

A. Misoriented invadopodia in ACs with ectopic expression of HLH-12. *zmp-1p::mCherry::MoesinABD* marks the AC. Photomicrographs show a WT AC with apical invadopodia and a +HLH-12 AC with basolateral invadopodia. Arrows: invadopodia, line: lack of invadopodia. n = 28 for each genotype.

B. Lack of vertical displacement in +HLH-12 ACs at the P6.pxx stage. ***p<0.001, Kolmogorov-Smirnov; n = 18 (WT) or 25 (+HLH-12). a.u., arbitrary units.

C. Ectopic expression of HLH-12 in the AC causes abnormal vulval development. Defective egg-laying (Egl), abnormal eversion of the vulva (Evl), or absence of a vulva (Vul) was observed in adults. There is no significant difference (n.s.) in the penetrance of abnormal vulval development observed in +HLH-12 and +HLH-12+LIN-32 hermaphrodites. Fisher's exact test; n = 20-25 for each genotype. All animals carry *lag-2p::2xnls-tagrfp* and *him-5(e1490).*

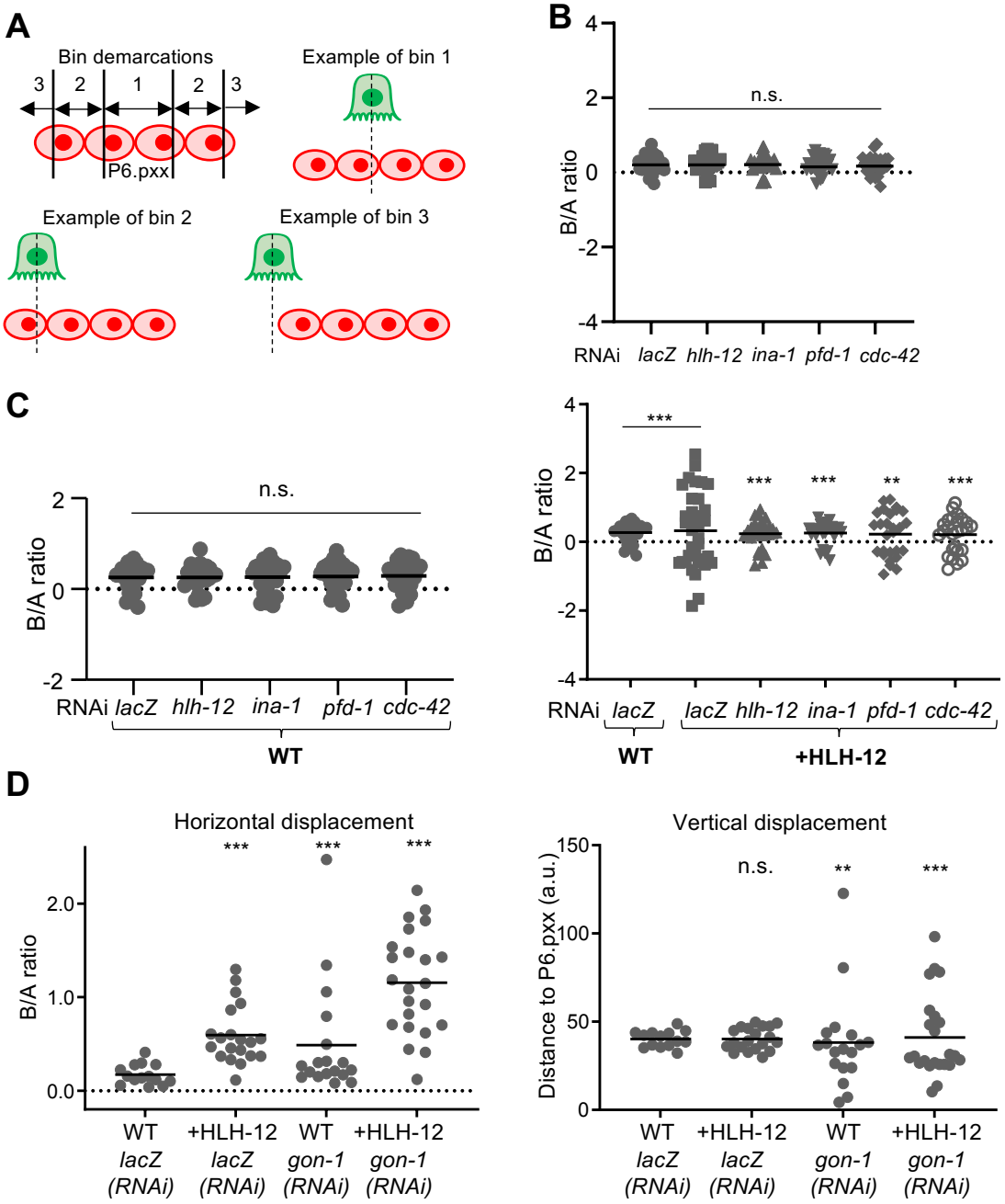

Figure S2

A. Detailed schematic of bins used to determine statistical significance of AC displacement in Figure 2. Animals were placed in bins according to the location of the center of the AC nucleus with respect to the P6.pxx nuclei. See Materials and Methods for more details.

B. RNAi against factors required for fDTC migration do not affect AC position per se. Animals lacking the +HLH-12 transgene were treated as in Figure 2E and no difference in position was seen from the *lacZ* RNAi negative control. As noted in the text, the AC position is on average slightly anterior to the midpoint of P6.pxx. See Materials and Methods for statistical details. n = 20-40, n.s. compared to *lacZ(RNAi).*

C. Second trial of RNAi against migration factors. See Materials and Methods and Figure S2A for bins; The statistics shown for the positive control and experimental RNAis are compared to +HLH-12 treated with *lacZ(RNAi).* n = 23-34 individuals. **p<0.01, ***p<0.001; when bar not shown, comparison is to +HLH-12+*lacZ(RNAi)*.

D. RNAi against *gon-1* disrupts the gonad and alters AC location in both WT and +HLH-12 animals. Note that horizontal displacement is quantified without regard to directionality. n = 20-25 for each genotype. Horizontal displacement: see Materials and Methods and Figure S1C for statistics used, ***p<0.001 compared to "WT" *lacZ(RNAi)*. Vertical displacement: Kolmogorov-Smirnov, **p<0.01, ***p<0.001 compared to WT+*lacZ(RNAi)*. Bars show mean.

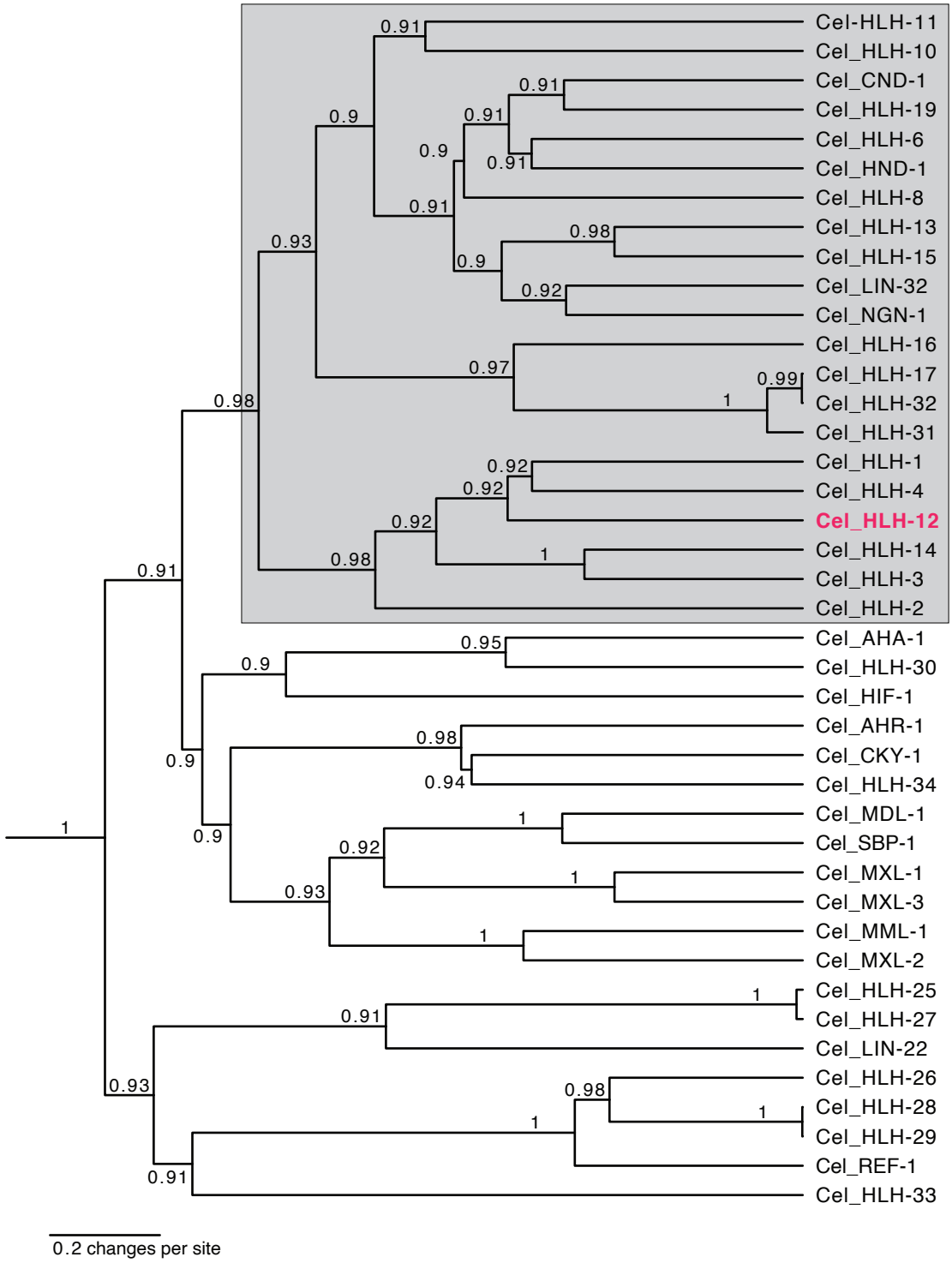

Figure S3
Phylogeny of 41 *C. elegans* bHLH proteins obtained with Bayesian Inference analysis (in BEAST with default parameters, 5 million generations, burnin 15%) of an ClustalW alignment of the bHLH domain of each protein (70 characters). Numbers on branches denote posterior probabilities. The grey box highlights the proteins that were used for further analysis (Figure 4).

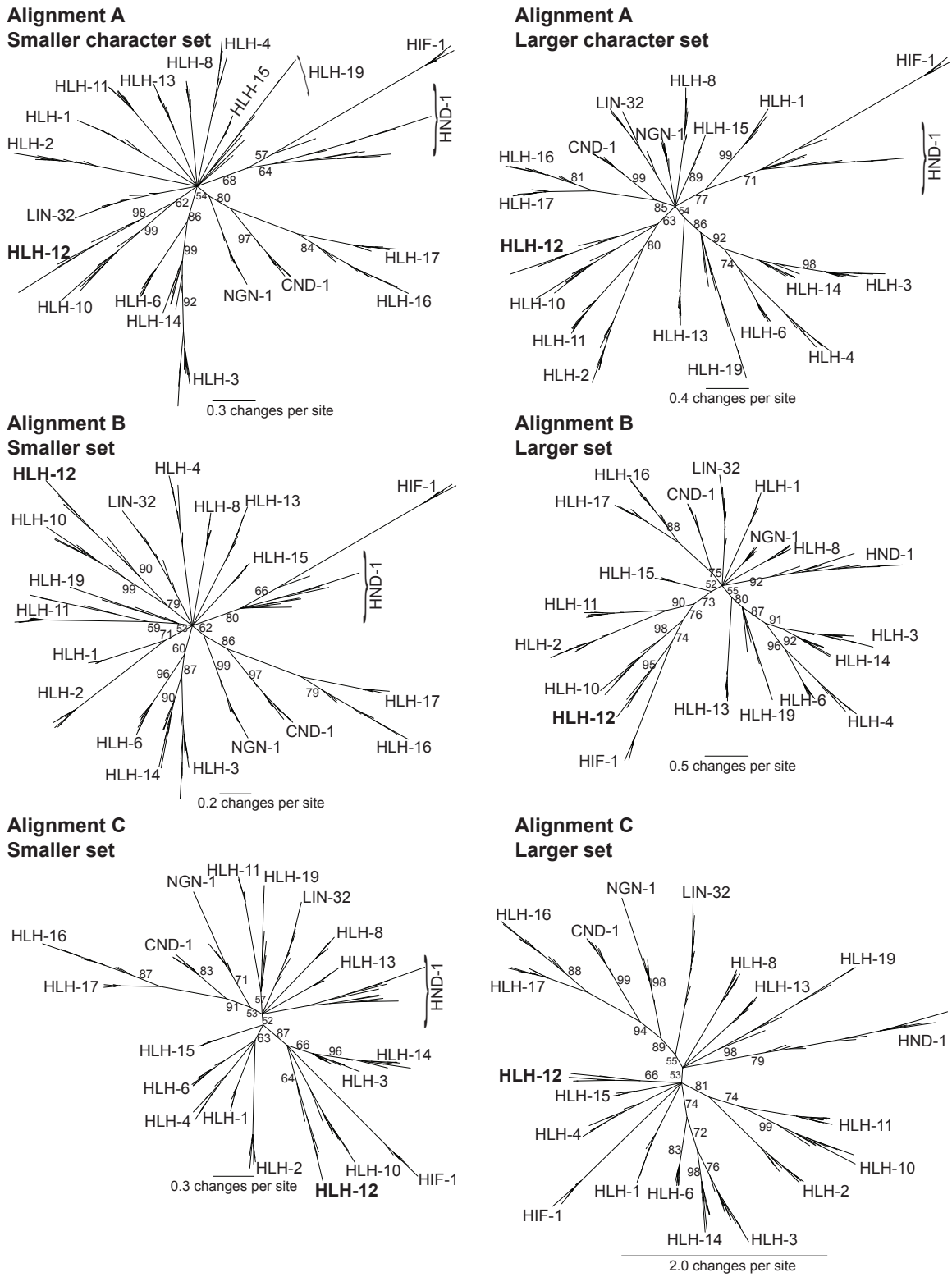

Figure S4

Unrooted phylograms from Bayesian Inference (BI) using two different character sets (a "smaller", minimal set of the most unambiguously aligned positions or a "larger" set that included characters in the smaller set and some flanking but more ambiguously aligned positions) from three different amino acid alignments: A (Clustal Omega alignment using default parameters, 86 or 228 characters), B (ClustalW alignment using default parameters, 73 or 199 characters), and C (ClustalW alignment using gap opening penalty set to 6, 79 or 223 characters). Individual taxa are not shown, as there is good evidence for the monophyly of ortholog groups, represented here by C. elegans names of bHLH proteins. Inferred protein sequences of bHLH genes are represented from *Oscheius tipulae, Heterorhabditis bacteriophora, Diploscapter coronatus, Caneorhabditis monodelphis, C. parvicauda, C. bovis, C. castelli, C. japonica, C. elegans* and *C. briggsae*. Clade credibility values (percentages of a bipartition appearing in 7,502 trees sampled from 3,750,000 post-"burn-in" trees) are only shown for internal branches if less than 100%. HLH-12 appears to be most closely related to HLH-10 in trees inferred from the least ambiguously aligned characters. HIF-1, on the other hand, shows unstable relationships with long-branch taxa such as HND-1, tending to cluster with HLH-12 and HLH-10 in alignments that include more ambiguously aligned characters.

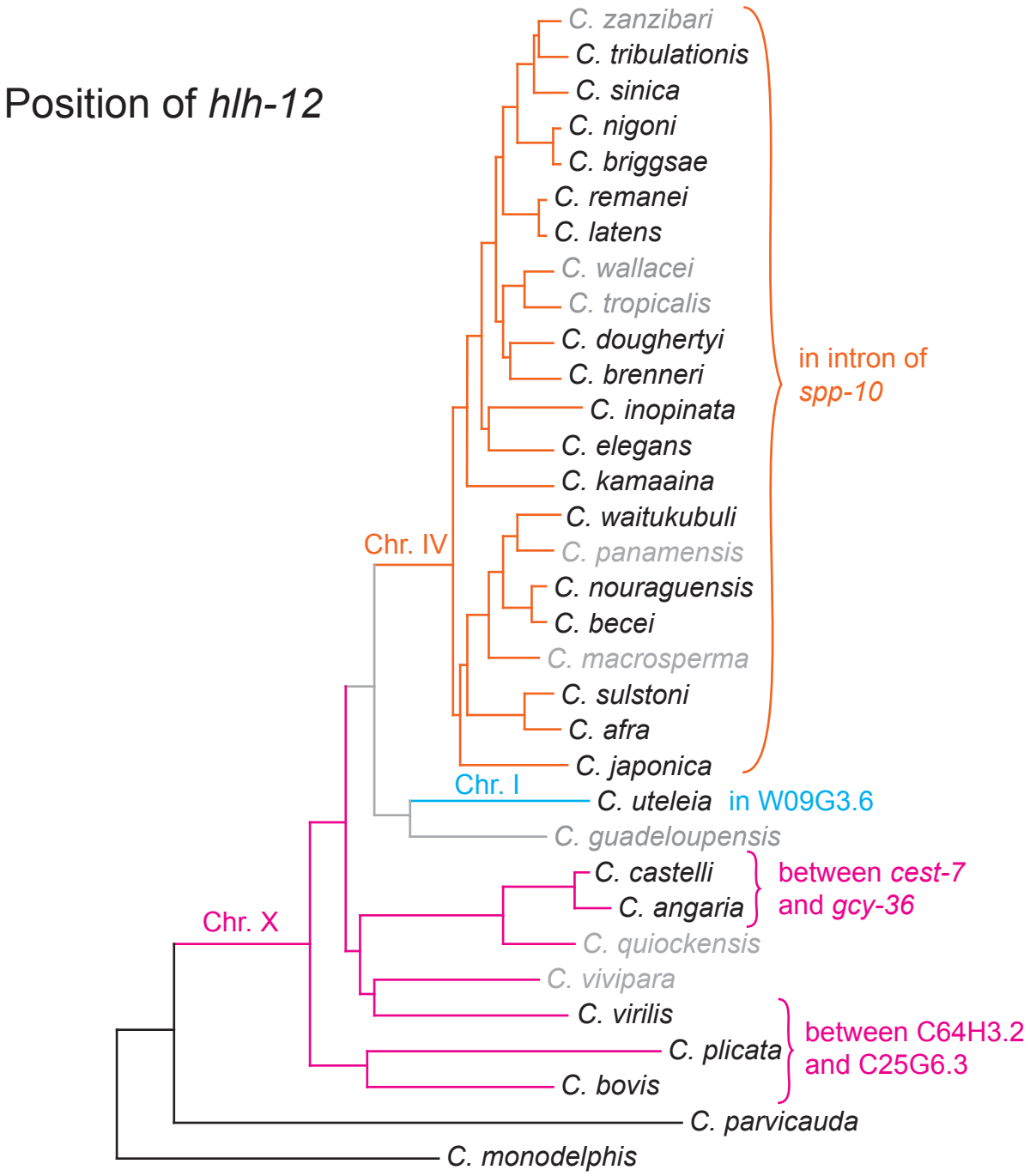

Figure S5
Presence of HLH-12 and the probable genomic location of its gene mapped onto the *Caenorhabditis* phylogram by (Stevens et al. 2020). All species except for *C. parvicauda* and *C. monodelphis* have HLH-12. Colored branches indicate the likely chromosomal location of *hlh-12* (pink: Chr. X; blue: Chr. I; orange: Chr. IV; grey: unknown). Names are greyed out of species for which the genes flanking *hlh-12* (and thus the chromosome) could not be determined.